Moroccan Journal of Chemistry
ISSN: 2351-812X
http://revues.imist.ma/?journal=morjchem&page=login
N. Mechbal / Mor. J. Chem. 4 N°4 (2016) 876-890

Experimental study of the corrosion inhibition of mild steel by the N1, N1, N5, N5-tetrakis ((1H-pyrazol-1-yl) methyl) naphthalene-1,5-diamine in hydrochloric acid solution

Naoual Mechbal[1], Yasser Karzazi[1,2*], Farid Abrigach[3], Fadoua El-Hajjaji[4] and Belkheir Hammouti [1]

[1] Laboratory of Applied Analytical Chemistry, Materials and Environment, Faculty of Sciences, University Mohammed Premier, P. O. Box 4808, 60046 Oujda, Morocco.
[2] LSIA, National School of Engineering and Applied Sciences, University Mohammed Premier, P. O. Box 3, 32003 Sidi Bouafif, ENSA Al Hoceima, Morocco.*
[3] Laboratory of Applied Chemistry and Environment (URAC 18), Faculty of Sciences, University Mohammed Premier, P. O. Box 4808, 60046 Oujda, Morocco.
[4]Laboratoire d'Ingénierie, d'Electrochimie, de Modélisation et d'Environnement (LIEME), Faculty of Sciences, University Sidi Mohammed Ben Abdellah, Fez, Morocco.

Abstract

The purpose of this study is to investigate the inhibition performance of N^1, N^1, N^5, N^5-tetrakis ((1H-pyrazol-1-yl) methyl) naphthalene-1, 5-diamine (NPD) on mild steel in 1 M HCl solution. The inhibitive action of this compound against the corrosion of mild steel in 1 M HCl solution has been investigated using weight loss measurements, Tafel Polarization and electrochemical impedance spectroscopy (EIS) techniques. The results obtained from the different corrosion evaluation techniques are in good agreement. Results obtained reveal that this compound performs excellently as corrosion inhibitor for mild steel in HCl 1M solution. The temperature effect on the corrosion behavior of mild steel in 1 M HCl with and without product at different concentrations was studied in the temperature range from 313 to 343 K. The adsorption free energy and activation parameters for the mild steel dissolution reaction were determined. Adsorption of this inhibitor on the mild steel surface in 1M HCl follows the Langmuir isotherm model. The surface characteristics of inhibited and uninhibited mild steel were investigated by scanning electron microscopy (SEM) and EDX studies. Quantum chemical approach, using the density functional theory (DFT)at B3LYP/6-31G (d,p) level, was realized in order to explain the inhibitory action and to get a better understanding about the relationship between the inhibition efficiency and molecular structure of NPD and the calculated quantum chemical parameters were discussed.

Corresponding author. E-mail : el.hajjajifadoua25@gmail.com
Recieved 29 Apr 2016,
Revised 10 Oct 2016,
Accepted 20 Dec 2016

Keywords: *Corrosion, Gravimetric, EIS, Adsorption, Langmuir isotherm, SEM, EDX, DFT.*

1. Introduction

Mild steel is the most widely used metal in industrial applications due to its excellent mechanical properties and low cost [1, 2]. Acids are used in industry during, chemical cleaning, of the scale in metallurgy [3], descaling, pickling, oil-well acidizing [4], petrochemical processes, erecting boilers, drums, heat exchangers, tanks and other electrochemical systems etc.., and this leads to a corrosive attack [1, 2]. The dissymmetry potentials between iron and hydrogen couples are the principal cause of this attack[5].Use of inhibitors is one of the most practical methods for protection against corrosion especially in acid solutions to prevent metal dissolution and acid utilization [6-8]. The effect of organic compounds containing heteroatom on the corrosion behavior of iron and steel in acidic solutions has been well documented and showed to be quite efficient to prevent corrosion and in addition to heterocyclic compounds containing polar groups and π-electrons cloud of the donor atoms and the metal surface with unoccupied d-orbitals [9, 10]. The synthesis of pyrazolic compounds permit easily to obtain several compounds of which the molecular structure contains several heteroatoms and several substituents [3, 4, 11]. The aim of present work is to extend these investigations by studying the inhibitive properties of N^1, N^1, N^5, N^5-tetrakis ((1H-pyrazol-1-yl) methyl) naphthalene-1, 5-diamine (NPD) on mild steel in 1 M HCl solution, is used to reduce corrosion rate of metal mainly by increasing or decreasing the anodic and/or cathodic reactions and decreasing diffusion rate for reactants to the surface of the metal and the electrical resistance of the metal surface. The corrosion of mild steel in hydrochloric acid has been monitored in the absence and presence of the new synthesized inhibitor for mild steel in 1 M HCl solution via the weight loss, electrochemical techniques such as potentiodynamic polarization and electrochemical impedance spectroscopy(EIS) and surface examination by scanning electron microscopy (SEM) and energy-dispersive X-ray spectroscopy (EDX) analysis which are employed to discuss the adsorption of pyrazolic based derivative inhibitor on mild steel surface. Theoretical chemistry including quantum chemical calculation has been proved to be a very powerful tool for studying the mechanism of corrosion inhibition [12]. This theoretical approach has been widely used to investigate a correlation between molecule structure and inhibition efficiency of an organic compound. Therefore, it is worthwhile to compute the structural parameters including the highest occupied molecular orbital energy E_{HOMO}, the lowest unoccupied molecular orbital E_{LUMO}, dipole moment (μ), $\Delta E = E_{HOMO} - E_{LUMO}$(energy band gap), absolute electronegativity (χ), global softness (S), fraction of electrons transferred (ΔN), back donation energy (ΔE_{b-d}), and global hardness (ω) were measured and discussed [13].

2. Materials and Methods

*2.1**Materials***

The Plate of mild steel (2cmx 2cm x 0.028cm) with a chemical composition (in (wt.%): of 0.09% P, 0.01% Al, 0.38% Si, 0.05% Mn, 0.21% C, 0.05% S and the remainder iron (Fe), clear with a series of abrasive paper 180 to 1200grade. After abrasion, the surface of the samples was rinsed in distilled water, in ethanol for grease and drying before use.

A solution of 1 M HCl was prepared by dilution of analytical grade HCl ≥ 37% with distilled water. For gravimetric measurements, the rectangular samples of size (2cm x 2cm x 0.028 cm) of mild steel were used for the corrosion testing. Prior to all measurements, the exposed area was mechanically abraded with 180, 320, 800, 1200 grades of emery papers. The specimens are washed thoroughly with double-distilled water, degreased with ethanol and dried before being weighed and immersed in 50 mL of the corrosive medium in the presence and absence of the inhibitor. The immersion time for the weight loss measurements was 6 hat 308K. At the end of immersion, the samples were cleaned and reweighted to determine the corrosion rate.

2.2 Characterization of N1, N1, N5, N5-tetrakis((1H-pyrazol-1-yl) methyl)naphthalene-1,5-diamine: NPD

The NPD used in the present study was synthesized in one step by simple condensation reaction between Hydroxypyrazole (4equiv) and diamine (1equiv) in the presence of Acetonitrile as solvent at reflux for 6h.The characterization data of the synthesized compound are as follows:**^{1}HNMR** (300 MHz, DMSO-d_6) δppm:7.80 (d, 4H, H $^{(3)}$ pz, J_{H-H} = 3 Hz); 7.48-7.20 (m,6H , H $^{(7)(8)(9)(12)(13)(14)}$) ; 6.80 (d, 4H,H $^{(1)}$ pz, J_{H-H} = 9 Hz); 6.22 (t, 4H, H $^{(2)}$ pz, J_{H-H} = 3 Hz); 5.62 (d, 8H, H $^{(4)}$, J_{H-H} = 6 Hz).**^{13}C NMR(**75 MHz, DMSO-d_6) δppm:142. 29 (C $^{(5)(10)}$); 138.66 (4C $^{(1)}$ pz); 128.94 (C $^{(3)}$ pz); 125. 40 (C $^{(6)(11)}$) ; 124. 17 (C$^{(7)(12)}$) ; 111. 10 (C$^{(9)(14)}$) ; 105. 85 (4C$^{(2)}$ pz) ; 60. 00 (4C$^{(4)}$).IR (KBr, ν (cm-1)) : 3444 - 2903 (CH) ; 1593 (C=N) ; 1435 (C=C) ; 1396 (C-N aromatique) ; 1145 (C-N aliphatique).

MS[M^{+}] (m/z):calculated 478. 56; found 501. 22 ([M^{+}+Na]).

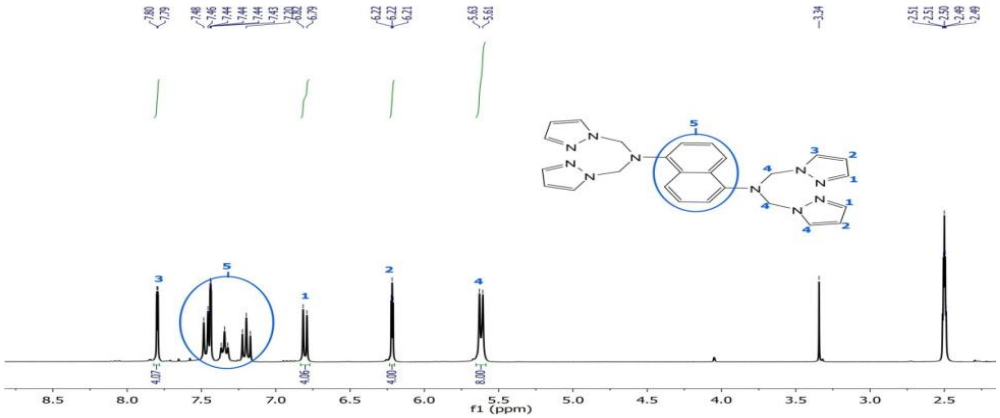

Figure 1.^{1}H NMR spectrum of N^1, N^1, N^5, N^5-tetrakis ((1H-pyrazol-1-yl) methyl) naphthalene-1, 5-diamine (NPD).

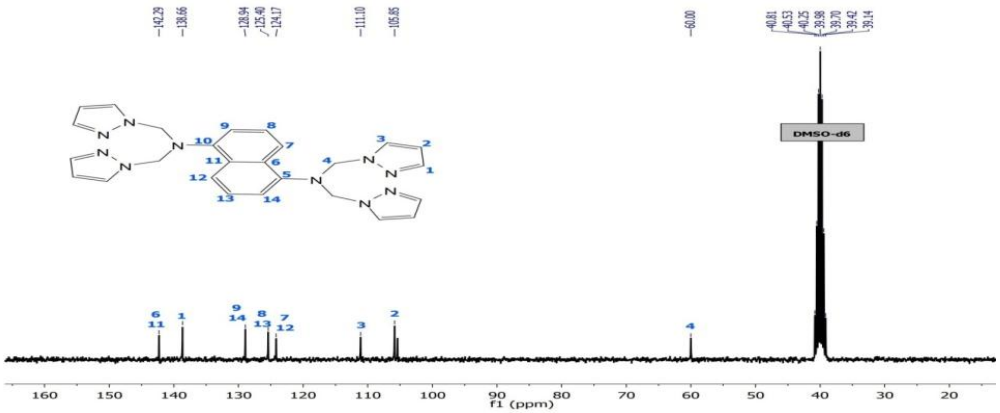

Figure 2.^{13}C NMR spectrum of N^1, N^1, N^5, N^5-tetrakis ((1H-pyrazol-1-yl) methyl) naphthalene-1, 5-diamine (NPD).

2.2 Weight loss measurement

The weight loss method is beneficial for monitoring inhibition efficiency due to its simple usage and reliability [14]. A previously weighted mild steel specimen were completely immersed in 50 ml of 1 M hydrochloric acid solutions without and with different concentrations of inhibitors and fixed the immersion time to 6 h at 308 K for the weight loss measurements [15].

2.3 Electrochemical measurements

In this work, we applied the technique of electrochemical impedance spectroscopy (EIS) to evaluate the protective

power of our inhibitor.The electrochemical measurements were carried out using a Volta lab (Tacussel- Radiometer PGZ 100) potentiostate and controlled by Tacussel corrosion analysis software model (Voltamaster 4). The electrochemical cell used had three electrodes: The reference electrode was a saturated calomel electrode (SCE). A platinum electrode was used as auxiliary electrode area of 1 cm^2. The working electrode is mild steel with a surface of 0.32 cm^2, the material used for constructing the working electrode was the same used for gravimetric measurements. All potentials given in this study were referred to this reference electrode. The working electrode was immersed in the test solution for 30 minutes at a study state to establish an open circuit potential (EPCO). After measuring EPCO, the electrochemical measurement were performed. All the electrochemical test were carried out in solutions aerated at 308K during experiment. The EIS was conducted in the frequency range with an supper limit of 100 kHz and different lower limit of mHz for the open circuit potential, with 10 points per decade, the resting potential, after 30 minutes of immersion in an acid, by application of 10 mV, an AC voltage peak to peak. Nyquist plot were made from these experiences. The best semicircle can be fit through the data point in the Nyquist plot using a nonlinear least squares fit so as to provide the intersections with the x-axis. ZView software version 2.8 was used to fit impedance data[16, 17].

2.4 Potentiodynamic polarization

Potentiodynamic polarization curves were obtained by changing the electrode potential automatically from -800 to -200 mV versus corrosion potential at a scan rate of 1 mV s^{-1}. All experiments were measured after immersion for 30 minutes in 1 M HCl in the absence and presence of inhibitor [18].

2.5 Scanning electron microscopy

The morphology of the corrosion products formed on the surface of the mild steel in 1M HCl solution in the absence and presence of 10^{-3} M of NPD were examined by SEM using a Traktor TN-2000 energy dispersive spectrometer and a Joel-Jem-1200 EX II electron microscope.

2.6 Quantum chemical calculations

Quantum mechanics study was carried out to determine the electron rich groups/atoms in a molecule as well as calculation of the HOMO and LUMO in order to give additional understandings on the likelihood of electron transfer between the inhibitor and metal. Quantum chemical calculations have been proved to be a powerful tool for studying corrosion inhibition mechanism [5, 15, 19-22]. The complete geometry optimization with no constraints of NPD as corrosion inhibitor was performed with DFT (density functional theory) based on Beck's three parameter exchange functional and Lee–Yang–Parr nonlocal correlation functional (B3LYP) [23-25] and the 6-31G(d, p) orbital basis sets for all atoms as implemented in Gaussian 09 program [26]. These calculations aim also to describe the interaction between the inhibitor molecule and the surface as well as the properties of this inhibitor concerning its reactivity.

2.7 Results and discussion

3.1Effect of NPD concentration and adsorption isotherm

The gravimetric data obtained in the absence and presence of different concentrations of the inhibitor N^1, N^1, N^5, N^5-tetrakis ((1H-pyrazol-1-yl) methyl) naphthalene-1, 5-diamine (NPD) of mild steel in 1M HCl are gathered in Table 1. The respective corrosion rate illustrated that the addition of (NPD) molecule decreases hugely the corrosion rate. The values obtained for the corrosion rate of mild steel in HCl in Table1 decrease with an increase of inhibition efficiency from 36.9 to 95.7% with the additionof$10^{-6}$to $10^{-3}$of (NPD)at a temperature of 308K. This increase in efficacy of inhibition is due to the adsorbed amount of the inhibitor that forms a film on the surface of metal also may be due to

the protonated form of nitrogen, which faster adsorbs to the surface of the mild steel. Indeed the molecule has a good inhibition of mild steel in acid 1M HCl as it contains aromatic rings planar benzene and pyrazole and contains N heteroatoms and π electrons. The inhibition efficiency IE % and surface coverage (θ) were determined by using the following equations:

$$\textbf{IE\%}= \frac{W°corr - Wcorr}{Wcorr} \times \qquad \textbf{(1)}$$

$$\theta = \frac{W°corr - I}{Wcor} \qquad \textbf{(2)}$$

Where Wcorr and W°corr are the corrosion rates of carbon steel in the presence and the absence of definite concentration of inhibitor, respectively, and θ is the degree of surface coverage of the inhibitor.

Table 1. Weight loss data of carbon steel in 1 M HCl for various concentrations of the NPD.

Inhibitor	Concentration (M)	Wcorr (mg.cm-2.h-1)	IE%	Θ
Blank	-	0.820	-	-
NPD	10-6	0.517	36.9	0.369
	10-5	0.412	49.8	0.498
	5.10-5	0.157	80.7	0.807
	10-4	0.087	89.3	0.893
	5.10-4	0.049	93.9	0.939
	10-3	0.035	95.7	0.957

From the results depicted in Table 1 it is observed that the IE% increases with increasing inhibitor concentration. The maximum value of IE% was obtained at 10^{-3} M concentration. Further increase in inhibitor concentration does not cause any significant change in the inhibition performance suggesting that 10^{-3}M is the optimum concentration. Increase in concentration, increases the effective surface coverage and therefore increases IE%. On the basis of increase in inhibition efficiency with increasing inhibitor concentration, it can be concluded that surface coverage and therefore inhibition efficiency increase with increasing inhibitor concentration. However, probably the maximum surface coverage was obtained at 10^{-3} M concentration. Therefore, further increase in the concentration did not cause any significant increase in the surface coverage and inhibition efficiency by inhibitor.

3.2 Adsorption isotherm

The adsorption isotherm can be determined by assuming that the inhibition effect was mainly due to adsorption at the metal/solution interface [1]and allows us to give more information about type of interaction between the inhibitor molecules and the mild steel surface. In this study, we found to fit the Langmuir adsorption isotherm [27] as shown in Fig. 4. Plotting C_{inh}/Θ versus C_{inh} yielded a straight line with a correlation coefficient (R^2) of 0.9999 and a slope close to 1.This suggests that the adsorption of NPD on metal surface followed the Langmuir adsorption isotherm according to the following equations [11, 13]:

$$\frac{C_{inh}}{\theta} = \frac{1}{K_{ads}} + C_{inh} \qquad \text{With} \qquad K=\frac{1}{55.5} e^{\left(-\frac{\Delta G°ads}{RT}\right)} \qquad (3)$$

Where *C* is the concentration of inhibitor, *K* is the adsorptive equilibrium constant; θis the surface coverage and ΔGads is the standard adsorption free energy. The value of the free energy of adsorption as calculated from Eq 3 is ΔGads = −40.3 kJ.mol^{-1} is found to be too negative indicating that NPD is strongly adsorbed on the steel surface and guaranteeing the spontaneity of the adsorption process and stability of the adsorbed layer on the steel surface are associated with chemisorption as a result of sharing or transfer of electron pair or π electrons from organic molecules to the metal surface to form a coordinate type of bond(chemisorption mechanism) [4, 28, 29]. Generally, a value of $\Delta G°$ads of −20 kJ mol^{-1} or less negative is associated with physical adsorption resulting from electrostatic interaction between a charged inhibitor and charged metal, and a value of $\Delta G°$ads of −40 kJ mol^{-1} or more negative is associated with chemical adsorption resulting from charged (electron) sharing between non-bonding electrons of the inhibitor and the d-orbitals of the surface Fe-atoms [30, 31].Hence, in our study the value of the free energy of adsorption indicates that our inhibitor NPD is adsorbed by a chemisorption mechanism [32].

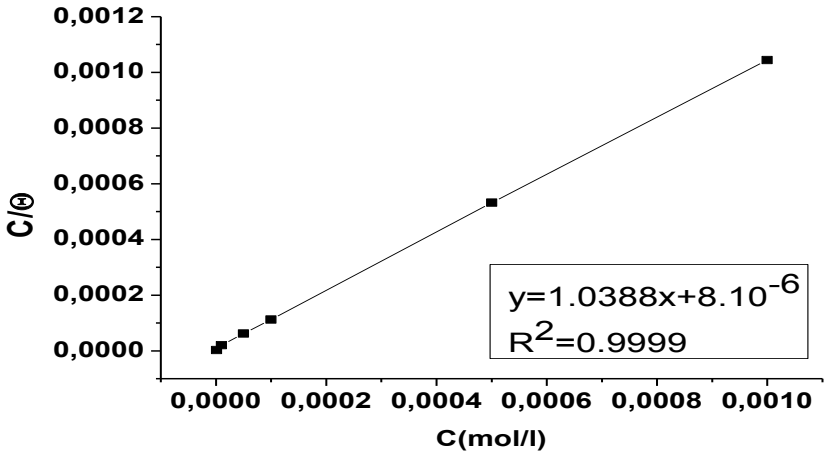

Figure1. Langmuir adsorption plot of NPD on mild steel in 1 M HCl at 308 K.

2.3 Effect of temperature

The study of effect of temperature was shown using weight loss measurement at various temperatures between313 K and 343 K in presence and in absence of NPD at 4h. The Fig 2 suggested that the inhibition efficiency was decreased from 93.8%to 83.7% with increase in temperature from 313 to 343 K. The increase in temperature accelerates the kinetics of the reaction and transport, this phenomenon may be due to desorption of inhibitor film. This study, allows us to draw more information on the thermodynamic parameters of activation and interpret the type of adsorption followed by the inhibitor and consequently the inhibition mechanism. The energy of activation is calculated using the Arrhenius equation Eq 4:

$$W_{corr}=A\, e^{-\frac{Ea}{RT}} \qquad (4)$$

Where Ea is the activation energy, R is the gas constant and A is the pre-exponential factor. Arrhenius plot for the corrosion rate of mild steel is given in Fig 2. Linear regression between log (W_{corr}) and 1/T is used to calculate the value of activation energy Ea for mild steel in 1 M HCl in the absence and presence of inhibitor. According to the results listed in Table 2, it was found that the value of Ea is higher for the inhibited solution than that for the uninhibited one. The higher value of Ea is obtained due to adsorbed inhibitor molecules on the most active adsorption sites (having the lowest energy) and the corrosion process takes place predominantly on the active sites of higher energy which create chemical barrier for charge and mass transfer [33], The activation parameters for the corrosion process were calculated from Arrhenius type plot according to the following equation Eq 5:

$$\mathbf{Wcorr}=\frac{RT}{\mathcal{N}h}e^{\frac{\Delta S°ads}{R}}e^{-\frac{\Delta H°ads}{R}} \quad (5)$$

Where h is Plank's constant, $\mathcal{N}$ is Avogadro's number, ΔS°ads is the entropy of activation and ΔH°ads is the enthalpy of activation. Arrhenius plots of (log W_{corr}) against (1/T) for mild steel in 1 mol L^{-1} HCl and plot of in (Wcorr/T) versus 1/T gave a straight line (Fig. 3a and 3b) with slope = $-\frac{\Delta H°ads}{R}$ and intercept Ln $(\frac{R}{\mathcal{N}.h})+\frac{\Delta S°ads}{R}$. The positive signs of change in enthalpy ΔH°ads reflected that the formation of the activated complex is exothermic process. Nature of the mild steel dissolution process is difficult, both in the absence and presence of the aqueous NPD [34]. The negative value of ΔS°ads implies that the activated complex represents an association rather than a dissociation step, this means that a decrease in disordering takes place on going from reactants to the activated complex [35-37], are shown in Fig 3a and 3b.

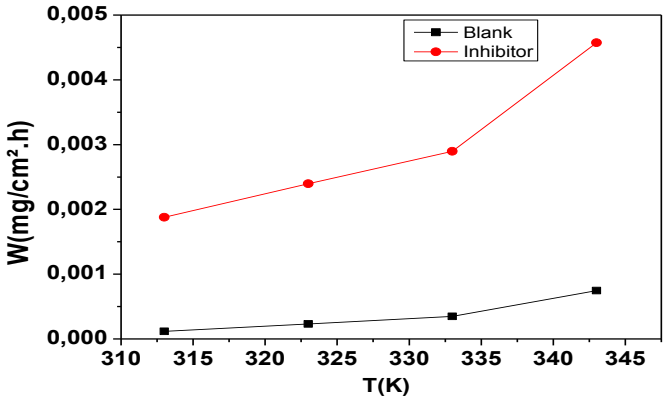

Figure 2. Relationship between corrosion rate and temperature for different concentrations of NPD.

The apparent activation energy obtained for the corrosion process in the free acid solution was found to be -25.39kJ mol^{-1}, and it was found to be -53.37 kJ mol^{-1} in the presence of the inhibitor. Inspection of the data show that the values of E_a and $\Delta H°_{ads}$ in the presence of the NPD are higher than those of pure acid indicating geometric blocking effect of adsorbed chemical species of the NPD on the metal surface [38]. Moreover, the average difference values of the (Ea -ΔH°ads) are 2.72 kJ/mol in absence and in presence of NPD, which are approximately equal to the average value of RT (2.63 kJ/mol) at 303K. This indicates that the corrosion process is a unimolecular reaction as it is characterized by the following equation:

$$Ea-\Delta H°ads=RT \quad \mathbf{(6)}$$

Table 2. Activation parameters for mild steel dissolution in 1 M HCl in the absence and presence of optimum concentration of NPD.

	Ea (KJ/mol)	ΔH°ads (KJ/mol)	ΔS°ads (KJ/mol)
Blank	25.4	22.7	-167.9
Inhibitor	53.4	50.6	-101.5

3. Electrochemical measurements

3.1. Electrochemical impedance spectroscopy (EIS)

This method consists of applying frequencies and low amplitude sinusoidal voltage wave to produce perturbation signals on the working electrode [20]. In order to acquire more information about corrosion mechanisms, the corrosion inhibition property of NPD on mild steel was examined by electrochemical impedance spectroscopy (EIS). Fig 4 show

the Nyquist diagrams of mild steel obtained at open circuit potential in 1 M HCl solution in the absence and presence of different concentrations of NPD, one single capacitive loop is observed on the Nyquist representations which means one phenomenon only occurred and this implies that the dissolution of mild steel is controlled by single charge transfer process [6, 20].

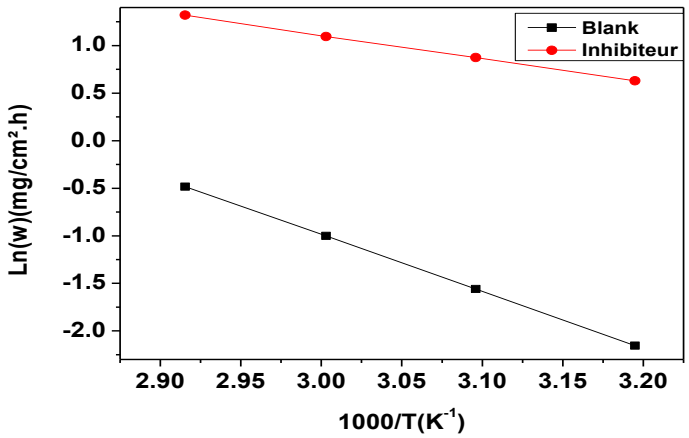

(a)

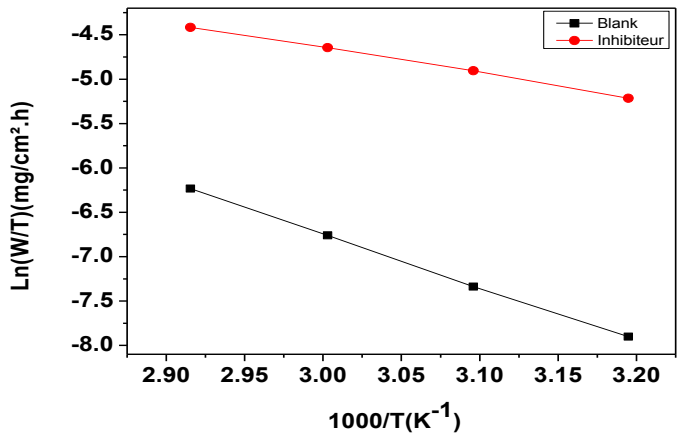

(b)

Figure 3. Arrhenius plots for mild steel in 1 M HCl in the absence and presence of different concentrations of NPD.

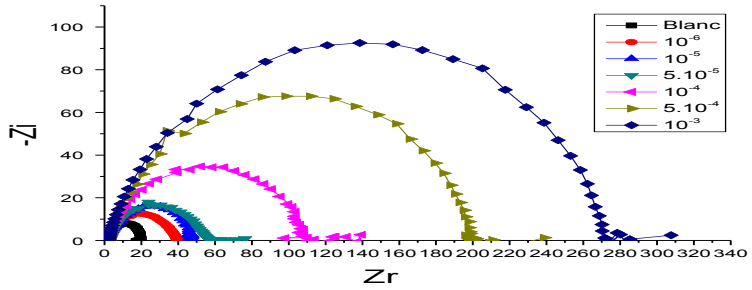

Figure 4. Nyquist diagrams for mild steel in 1 M HCl at different concentrations of NPD at 308 K

Inspection of data in the Table 3 clearly shows that in the whole concentration range, the value of the polarization resistance R_{ct} increases with the concentration of NPD and reached a maximum value of 277.2 Ω cm^2 at 10^{-3} M. A large polarization resistance is associated with a slower corroding system, which indicates the improvement in inhibiting effect on mild steel corrosion this effect is connected with simultaneous decrease of the double-layer for

example, the double layer capacitance (C_{dl}) value decrease from 321.2 µF cm^{-2} in the blank solution to 57.4 µF cm^{-2} in the case of 10^{-3} M of NPD, signifying that the charge and discharge rates to the metal–solution interface is greatly decreased. A simple Randles circuit in Fig 4 fit the impedance spectra. Where Rs is the solution resistance, R1 denotes the charge-transfer resistance and CPE1 is constant phase element. The introduction of CPE1 into the circuit was necessitated to explain the depression of the capacitance semicircle, which corresponds to surface heterogeneity resulting from surface roughness, impurities and adsorption of inhibitors [6]. The CPE1impedance of this element is frequency-dependent and can be calculated using the Eq 7[15, 18]:

$$Z_{CPE}=\frac{1}{Q(jw)^n} \quad (7)$$

Where Q is the CPE constant (in Ω^{-1} S cm^{-2}), ω is the angular frequency (in rad s^{-1}), j^2 = -1 is the imaginary number and n is a CPE1 exponent which can be used as a gauge for the heterogeneity or roughness of the surface.

Table 3. Impedance parameters for corrosion of mild steel for selected concentrations of NPD in 1M HCl at 308K.

Inhibitor	Concentration (M)	R1 (Ω.cm²)	Cdl (µF.cm^{-2})	IE%
Blank	1	19.83	321.2	-
NPD	10^{-6}	40.33	98.7	50.8
	10^{-5}	46.96	84.8	57.7
	5.10^{-5}	60.55	52.6	67.3
	10^{-4}	116.8	54.5	83
	5.10^{-4}	205.8	61.9	90.4
	10^{-3}	277.2	57.4	92.9

A simple Randles circuit in Fig 5 fit the impedance spectra. Where Rs is the solution resistance, R1 denotes the charge-transfer resistance and CPE1 is constant phase element. The introduction of CPE1 into the circuit was necessitated to explain the depression of the capacitance semicircle, which corresponds to surface heterogeneity resulting from surface roughness, impurities and adsorption of inhibitors [6]. The CPE1impedance of this element is frequency-dependent and can be calculated using the Eq 7[15, 18]:

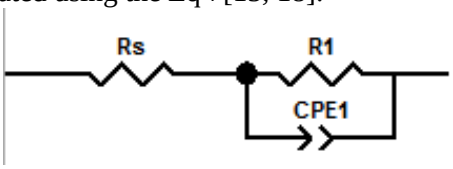

Figure 5. Electrical equivalent circuit used to fit the EIS experimental data.

In addition, the double layer capacitances, C_{dl}, for a circuit including a CPE1 were calculated by using the following Eq 8:

$$C_{dl}=\frac{1}{\omega * R1} \quad (8)$$

Where$\omega=2\pi f_{max}$

With C_{dl}: Double layer capacitance (µF.cm^{-2}); f_{max}: maximum frequency (Hz) and R1: Charge transfer resistance (Ω.cm^2). The inhibition efficiency is calculated from the R1 values using the following Eq 9 [39]:

$$IE\%=\frac{R1-R°1}{R1}\times 100 \quad (9)$$

Where R°1 and R1are the charge transfer resistances without and with various concentrations of inhibitors

respectively. InTable3, it can be seen from the results that the values of R1 significantly increase whereas the values of C_{dl} decrease in the presence of NPD. This increase in R1 and decrease in C_{dl} values in the presence of studied inhibitor are attributed to a decrease in local dielectric constant and/or to an increase in the thickness of the electrical double layer [6].

3.1 Potentiodynamic polarization

Tafel polarization curves for mild steel in 1 M HCl for different concentrations of NPD at 308 K are shown in Fig 6. The related electrochemical parameters such as corrosion potential (E_{corr}), corrosion current density (I_{corr}), and Tafel cathodic and anodic constants (β_c and β_a) were listed in Table 4. The I_{corr} was determined by Tafel extrapolation of the cathodic and the anodic polarization curves. The values of IE% were calculated using the following Eq 10 [7].

$$\mathbf{IE\%} = \frac{Icorr - Icorr(i)}{Icorr} \times 100 \qquad \mathbf{(10)}$$

Where I_{corr} and I_{corr} (i) are the corrosion current densities for mild steel electrode in the uninhibited and inhibited solutions, respectively.

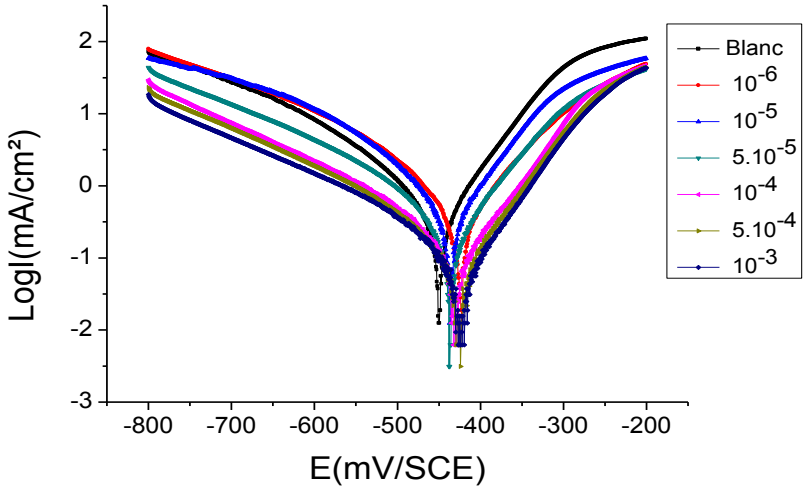

Figure 6. Polarization curves of carbon steel in 1 M HCl for various concentrations of NPD at 308K.

The Fig.6 shows the cathodic and anodic polarization plots of mild steel immersed in 1 M HCl at 308 K in the absence and presence of different concentrations of NPD. It is evident from Fig 6 that both reactions were suppressed with the addition of NPD used in the study, suggesting that NPD reduced the anodic dissolution reactions and retarded the hydrogen evolution reactions on the cathodic sites. Electrochemical parameters such as corrosion potential (E_{corr}), cathodic and anodic Tafel slopes (β_c and β_a) and corrosion current density (I_{corr}) were obtained by extrapolation of the anodic and cathodic regions of the Tafel plots and inhibition efficiency is listed in Table 4. It is evident from Table 4 that the value of β_a changed with increase in the presence of NPD whereas more pronounced change occurs in the values of βc indicating that both anodic and cathodic reactions are effected but effect on the cathodic reactions is more prominent. The shift in the anodic Tafel slope (β_a) is due to the inhibitor molecules adsorbed on the metal surface. An inhibitor can be classified as an anodic or cathodic type when the change in E_{corr} value is larger than 85 mV. In the present study, the maximum displacement was 27.6 mV cathodically when compared to the blank [40]. The reduction of anodic and cathodic currents in presence of NPD can be explained by the blocking of active sites with the formation of a protective film on the electrode surface [41].

Table 4. Corrosion parameters for corrosion of mild steel with selected concentrations of NPD in 1M HCl by Potentiodynamic polarization method at 308K.

Inhibitor	Concentration (M)	$-E_{i=0}$ (mV/SCE)	Icorr (m A/cm²)	-βc (mV/dec)	βa (mV/dec)	IE %
Blank	1	450.8	0.4132	84.5	65	-
NPD	10^{-6}	431.3	0.2411	73.1	66.6	41.6
	10^{-5}	437.3	0.1782	47.9	45.2	56.9
	5.10^{-5}	437.3	0.1609	80.9	70.4	61.06
	10^{-4}	431.2	0.0677	72.4	66.6	83.6
	5.10^{-4}	426.2	0.0523	75	61.9	87.3
	10^{-3}	423.6	0.0397	63.3	59	90.4

The data in Table 4 show that increasing NPD concentration, the values of corrosion potential (E_{corr}) shifted to negative direction indicating that it acts as mixed type inhibitor. The obtained results show that the inhibition efficiency increased with increasing the inhibitor concentration reaching a maximum value at 10^{-3} M in both cases of inhibitors, while the corrosion current density (I_{corr}) decreased when the concentration of NPD is increased. This could be explained on the basis of adsorption of NPD on the mild steel surface and the adsorption process increased with enhancing inhibitor concentration and also hindered attack on the mild steel electrode by acid. The results of electrochemical measurements agreed well with those of weight loss studies with the slight deviation in the values. Variation in the immersion period of mild steel in1 M HCl is the reason for the observed deviation.

4 . Morphological investigation

4.1Scanning electron microscopy analysis

In order to evaluate the conditions of the steel surfaces in contact with hydrochloric acid solution, samples were imaged in the SEM.

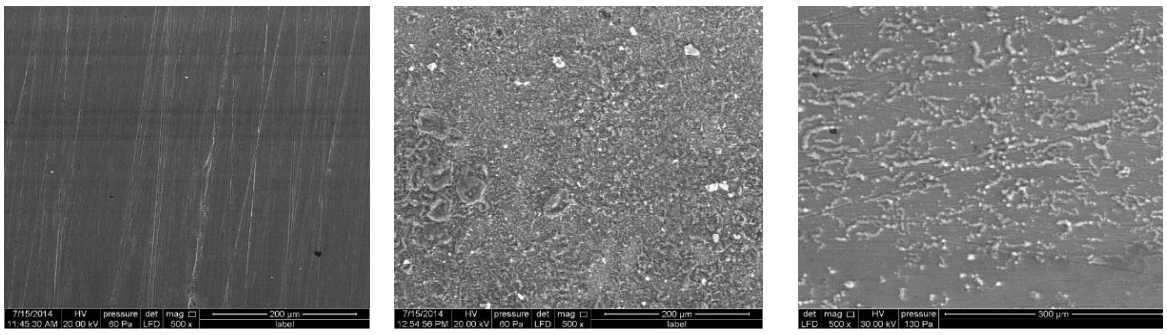

A **B** **C**

Figure 7. SEM micrographs of mild steel samples at 308 K (A) only surface polishing, (B) after immersion in 1 M HCl without inhibitor, (C) after immersion in 1 M HCl + 1.0×10^{-3} M NPD.

Surface was observed before and after 6h of immersion in 1 M HCl in the absence and presence of inhibitor at 308 K.The SEM image surface of steel after immersion in 1 M HClFig.7 (B) this reveals a severe damage on surface due to metal dissolution. In the presence of the NPD (Fig. 7C), a smooth surface can be observed, confirms that the extract prevents the corrosion of mild steel through adsorption of the inhibitors on metal surface in comparison to the blank.

These results corroborate the results from the electrochemical impedance spectroscopy and weight loss experiments [14, 18].

4.2EDX analysis

The EDX spectra in the absence and the presence of the optimum concentration of the NPD after 6 h immersion are shown in Fig 8. The EDX spectrum without NPD gives signals only for carbon (C) and Fe as shown in Fig. 5a. However, the EDX spectra of mild steel in the presence of NPD (Fig. 8a–b) showed characteristics signal for N and O along with C and Fe. The EDX spectra showed an additional signal for the existence ofN element (due to the nitrogen atoms of the inhibitors) the EDX spectra suggests that NPD inhibit mild steel corrosion by adsorbing on the mild steel surface[10, 42].

(a)

(b)

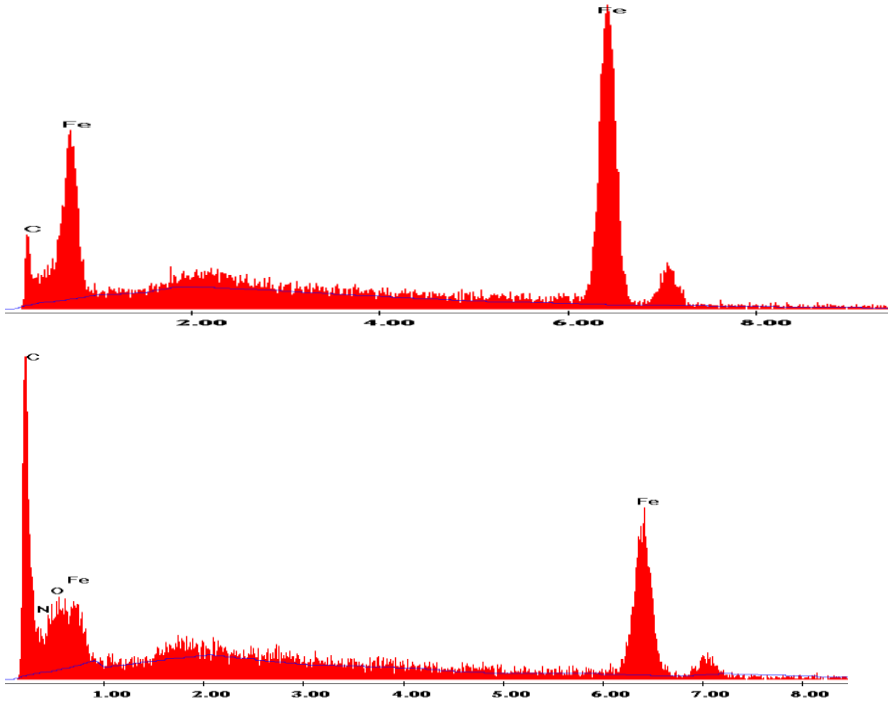

Figure8. EDX spectra of mild steel surfaces the mile steel and in the absence (a)and presence of optimum concentration of NPD (b).

5. Quantum chemical calculations

The optimized geometry at the B3lyp/6–31g (d, p) level of NPD and its corresponding frontier molecular orbitals (HOMO and LUMO) are shown in Fig 9. The energy levels viz, E_{HOMO}, E_{LUMO} and ΔE calculated in atomic units (u.a. or Hartree) are presented in Table 5.The HOMO and LUMO are important to investigate because they offer an indication about the regions of the molecule with the propensity to give or receive electrons. From Fig 9, the HOMO and LUMO are mainly localized on the naphthalene structure and the nitrogen atoms of the amine groups. The presence of the nitrogen atoms of the amine groups break the planarity of the molecule NPD and thus prevents the HOMO and LUMO to be delocalized on the entire molecule. The calculated Mulliken charges on the atoms provide additional information on the reactivity sites. The highest negative charges are found on the nitrogen atomsN24(-0.507) and N7 (-0.494) followed by the nitrogen atoms of the triazole rings which bear quite high negative charges around -0.26 to -0.30, indicating that all these nitrogen atoms are the atoms on which the electrophilic attack would preferably occur.

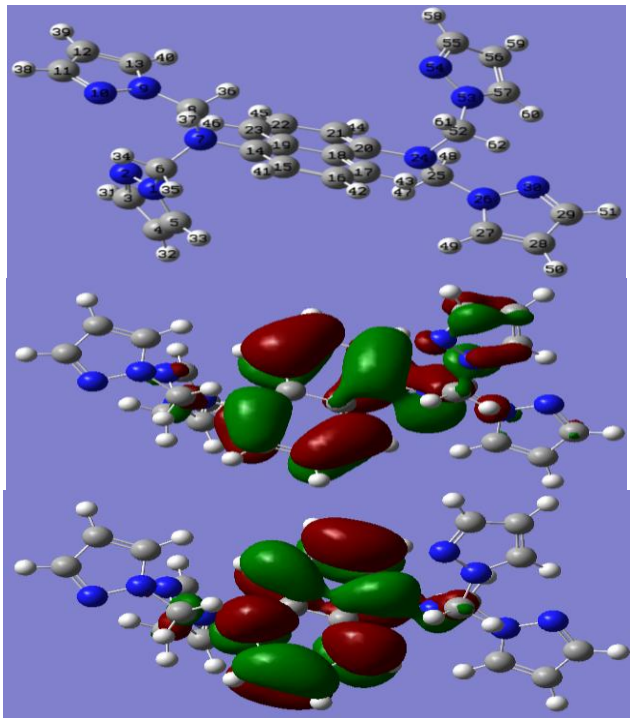

Figure 9. Optimized geometry, HOMO and LUMO of the inhibitor molecule (NPD).

An ideal corrosion inhibitor has a greater tendency to receive electrons, donate electrons or bind strongly to the metal surface [3] which suggests that NPD may donate electrons to the electrode surface through HOMO (naphthalene structure and nitrogen atoms of the amine groups) and accept electrons from the electrode surface through LUMO (naphthalene structure). Also, the value of E_{HOMO} for NPD inhibitor was found to be-0.04719a.u, which was higher (less negative) compared to that of the iron values (-0.20181, -1.00063, and -1.76592 a.u.). The literature shows that E_{HOMO} is frequently associated with the electron donor ability of the molecule and the inhibition efficiency increases with increase in the values of E_{HOMO}. A higher value of E_{HOMO} for NPD than of iron suggests that it has a greater potential to give electrons [42]. From Table5, it is clear that the energy gap values follow the order, Fe^{3+}>Fe^{2+}>NPD>Fe. Which suggested that NPD has an ability to donate electrons preferably to Fe^{3+} and Fe^{2+}. So, the molecular modeling shows the corrosion inhibition potential of NPD while its possible mode of interaction with metal surface. In acidic solution, the nitrogen atoms of NPD bearing high negative charges may easily contribute to formation of a coordinate bond between unshared electron pairs of unprotonated nitrogen atoms of the inhibitor and vacant d-orbitals of metal surface atoms. This scenario is in good agreement with the fact that chemisorption mechanism is more likely to occur (ΔG_{ads} = −40.3 kJ.mol^{-1}). Further, the nitrogen atoms of NPD can be protonated easily, due to high electron density on it, leading to positively charged inhibitor species. The adsorption can occur via electrostatic interaction between positively charged inhibitor molecules and negatively charged metal surface leading to physisorption of the inhibitor molecules [15].

Table 5. Calculated quantum chemical parameters for CPEPB and iron (Fe, Fe^{2+} and Fe^{3+}).

Compound	E_{HOMO} (a.u.)	E_{LUMO} (a.u.)	$\Delta E = E_{LUMO} - E_{HOMO}$ (a.u.)
NPD	-0.04719	-0.21206	0.16487
Fe	−0.20181	−0.12376	0.07805
Fe^{2+}	−1.00063	−0.70608	0.29455
Fe^{3+}	−1.76592	−1.12498	0.64094

6.Conclusion

1. NPD acts as a fairly good inhibitor for carbon steel in 1.0 M HCl solution.

2. The efficiency of inhibition by NPD increases with increasing concentration of the inhibitor, but decreases with increasing temperature.

3. Results obtained from polarization and impedance studies show that the percentage inhibition efficiency increases as concentration increases.

4. Polarization studies reveal that NPD act as a mixed-type inhibitor.

5. The SEM and EDX study well support the adsorption of NPD and the images confirm the formation of the protective layer on the metal surface.

6. NPD possibly will offer electrons to the electrode surface through HOMO (naphthalene structure and the nitrogen atoms of the amine groups) and receive electrons from the electrode surface through LUMO (naphthalene structure).

Acknowledgment

Prof. Y. KARZAZI extends his appreciation to the Laboratory for Chemistry of Novel Materials, University of Mons, Belgium, for access to the computational facility.

References:

[1] P. Singh, M. A. Quraishi, S. L. Gupta, A. Dandia, 10 (2016) 139-147.

[2] B. Xu, Y. Liu, X. Yin, W. Yang, Y. Chen, Sci., 74 (2013) 206-213.

[3] E. E. Ebenso, I. B. Obot, 5 (12) (2010) 2012-2035.

[4] K. M. Hijazi, M. Abdel-Gaber, G. O. Younes, Int. J. Electrochem. Sci, 10 (2015) 4366-4380.

[5] M. El Alaoui Belghiti, M. Dahmani, M. Messali, Y. Karzazi, A. Et-Touhami, A. Yahyi, A. Dafali, B. Hammouti, Der Pharma Chem., 7 (5) (2015) 106-115.

[6] H. Lgaz, R. Salghi, M. Larouj, M. Elfaydy, S. Jodeh, Mor. J. Chem. 4 (2)(2016) 592-612.

[7] R. Salghi, L. Bazzi, B. Hammouti, S. Kertit, A. Bouchtart, Z. El Alami, Ann. Chim. Sci. Matér., 25(2000)593-600.

[8] N. S. Patel, J. Hadlicka, P. Beranek, R. Salghi, H. Bouya, H. A. Ismat, B. Hammouti, Port. Electrochimica Acta, 32 (6) (2014) 395.

[9]C. Verma, M. A. Quraishi, A. Singh, J. Taibah Univ. Sci., 10 (5) (2016)718-733.

[10] M. Bouklah, B. Hammouti, M. Lagrenée, F. Bentiss, Corrosion Science, 48 (9) (2006) 2831-2842

[11] A. Al Maofari, G. Ezznaydy, Y. Idouli, F. Guédira, S. Zaydoun, N. Labjar, S. El Hajjaji, J. Mater. Environ. Sci. 5 (2014) 2081- 2085.

[12] D. Daoud, T. Douadi, H. Hamani, S. Chafaa, M. Al-Noaimi, Corros. Sci. 94 (2015) 21-37.

[13] M. Elbelghiti, Y. Karzazi, A. Dafali, B. Hammouti, F. Bentiss, I. B. Obot, I. Bahadur, E. E. Ebenso, J. Mol. Liq., 218 (2016) 281-293.

[14] N. O. Obi-Egbedi, I.B. Obot, S. A. Umoren, Arab. J. Chem., 5 (2012) 361-373.

[15] A. Bousskri, A. Anejjar, M. Messali, R. Salghi, O. Benali, Y. Karzazi, S. Jodeh, M. Zougagh, E. E. Ebenso, B. Hammouti, J. Mol. Liq. 211 (2015) 1000-1008.

[16] Y. ELouadi, F. Abrigach, A. Bouyanzer, R. Touzani, O. Riant, B. ElMahi, A. El Assyry, S. Radi, A. Zarrouk, B. Hammouti, Der Pharma Chemica, 7(8) (2015) 265-275.

[17] S. El Arrouji, K. I. Alaoui, A. Zerrouki, S. El Kadiri, R. Touzani, Z. Rais, M. F. Baba, M. Taleb, A. Chetouani, A. Aouniti, J. Mater. Environ. Sci. 7 (1) (2016) 299–309.

[18] K. R. Ansari, M. A. Quraishi, J. Assoc. Arab Univ. Basic Appl. Sci., 18 (2015) 12-18.

[19] Y. Karzazi, M. E. Belghiti, F. El Hajjaji, B. Hammouti, J. Mater. Environ. Sci. 7 2016 3916-3929.
[20] A. Khadraoui, A. Khelifa, H. Boutoumi, Y. Karzazi, B. Hammouti, S.S. Al-Deyab, Chemical Engineering Communications, 203 (2) (2016) 270-277.
[21] Y. Karzazi, M.E. Belghiti, A. Dafali, B. Hammouti, J. Chem. Pharm. Res. 6 (2014) 689-696.
[22] F. El-Hajjaji, B. Hammouti, Y. Karzazi,LAP Lambert Academic Publishing Ed. ISBN 978-3-659-52951-1, Chaps 1-6, pages 130.
[23] A.D. Becke, J. Chem. Phys. 96 (1992) 9489-9497.
[24] A.D. Becke, J. Chem. Phys. 98 (1993) 1372-1377.
[25] C. Lee, W. Yang, R.G. Parr, Phys. Rev. B 37 (1988) 785-789.
[26] M.J. Frisch, G. W. Trucks, H. B. Schlegel, G. E. Scuseria, M.A. Robb, J. R. Cheeseman, G. Scalmani, V. Barone, B. Mennucci, G. A. Petersson, H. Nakatsuji, M. Caricato, X. Li, H. P. Hratchian, A. F Izmaylov, J. Bloino, G. Zheng, J. L. Sonnenberg, M. Hada, M. Ehara, K. Toyota, R. Fukuda, J. Hasegawa, M. Ishida, T. Nakajima, Y. Honda, O. Kitao, H. Nakai, T. Vreven, J. A. Montgomery, Jr., J. E. Peralta, F. Ogliaro, M. Bearpark, J.J. Heyd, E. Brothers, K. N. Kudin, V. N. Staroverov, R. Kobayashi, J. Normand, K. Raghavachari, A. Rendell, J. C. Burant, S.S. Iyengar, J. Tomasi, M. Cossi, N. Rega, J. M. Millam, M. Klene, J.E. Knox, J.B. Cross, V. Bakken, C. Adamo, J. Jaramillo, R. Gomperts, R. E. Stratmann, O. Yazyev, A. J. Austin, R. Cammi, C. Pomelli, J. W. Ochterski, R. L. Martin, K. Morokuma, V.G. Zakrzewski, G.A. Voth, P. Salvador, J. J. Dannenberg, S. Dapprich, A.D. Daniels, Ö. Farkas, J.B. Foresman, J.V. Ortiz, J. Cioslowski, D.J. Fox, Gaussian, Inc. Wallingford CT, (2009).
[27] K. Boumhara, M. Tabyaoui, C. Jama, F. Bentiss, J. Ind. Eng. Chem., 29 (2015) 146-155.
[28] F. Touhami, A. Aouniti, Y. Abed, B. Hammouti, S. Kertit, A. Ramdani, K. Elkacemi, 42 (2000) 929-940.
[29] M.J. Bahrami, S.M.A. Hosseini, P. Pilvar, Corros. Sci. 52 (2010) 2793-2803.
[30] A. H. Al Hamzi, H. Zarrok, A. Zarrouk, R. Salghi, B. Hammouti, Int. J. Electrochem. Sci, 8 (2013) 2586-2605.
[31] S. Manimegalai, P. Manjula, J. Mater. Environ. Sci. 6 (6) (2015) 1629-1637.
[32] M. Behpour, S.M. Ghoreishi, N. Mohammadi, N. Soltani, M. Salavati-Niasari, Corros.Sci. 52 (2010) 4046-4057.
[33] I. Ahamad, R. Prasad, M. A. Quraishi, J. Solid State Electrochem. 14 (2010) 2095-2105.
[34] L. Herrag, B. Hammouti, S. Elkadiri, A. Aouniti, C. Jama, H. Vezin, F. Bentiss, Corr. Sci. 52 (2010) 3042–3051.
[35] C. Verma, M. A. Quraishi, Ain Shams Eng. J., 7 (1) (2016) 1-9.
[36] C. B. Verma, P. Singh, M. A. Quraishi, J. Assoc. Arab Univ. Basic Appl. Sci., 21 (2016) 24-30.
[37] M. E. Belghiti, Y. Karzazi, A. Dafali, I. B. Obot, E. E. Ebenso, K. M. Emran, I. Bahadur, B. Hammouti, F. Bentiss, J. Mol. Liq., 216 (2016) 874-886.
[38] S.K. Saha, P. Ghosh, A. Hens, N.C. Murmu, P. Banerjee, Phys. E: Low-dimensional Syst. Nanostructures, 66 (2015) 332-341.
[39] A. El Assyry, R. Jdaa, B. Benali, M. Addou, A. Zarrouk, J. Mater. Environ. Sci. 6 (9) (2015) 2612-2623.
[40] N. O. Eddy, B. I. Ita, J. Molecular Modeling 17 (2) (2011) 359-376.
[41] M. Bourass, A. T. Benjelloun, M. Benzakour, M. Mcharfi, M. Hamidi, 6 (2015) 1542-1553.
[42] H. Hoptop, W.C. Lineberger, Phys. Chem. Ref. Data, 14 (1985) 731-750.